Nonlinear Harmonic Monitoring of Gouged Dents in Cyclically Loaded Pipeline Specimens

Alfred E. Crouch, PE and G. Graham Chell, PhD
Southwest Research Institute®
6220 Culebra Road
San Antonio, Texas 78238

ABSTRACT

There is currently no in-line inspection technology for quantitative evaluation of gouged dents other than geometry (caliper) pigs. Southwest Research Institute (SwRI®), under sponsorship of the U.S. Pipeline and Hazardous Materials Safety Administration (PHMSA), is evaluating the nonlinear harmonic method to provide severity ranking for gouged dents; even dents that have been re-rounded by internal pressure. This paper describes experiments with four pressure chambers made from 12-inch line pipe. Internal scanner hardware, driven from the outside under computer control, deploys nonlinear harmonics probes against the pipe inner surface. Data collected represents residual strain patterns on the pipe surface and can be analyzed to indicate the length, width, and depth of the outside gouge. The chambers, each containing several mechanical damage defects, are being cyclically loaded until all defects fail.

BACKGROUND

The statistics of pipeline incidents are well known, including the fact that mechanical damage is a major cause of reported incidents. This significance of the outside force cause of incidents has prompted funding agencies to make investment in R&D for detection and characterization of that type of defect. However, it should be pointed out that detection of outside force defects by in-line means will *not* prevent the 70 to 80 percent of such defects that fail immediately upon their initiation. So the target for in-line detection of outside force defects is the 10 percent or so of delayed failures. Even though this target is a small fraction of the total pipeline incidents, it can nevertheless have tragic consequences such as the failure in Bellingham, WA, in 1999.

For several years, SwRI has been involved in a project to refine a detection method for mechanical damage defects, under sponsorship of the U.S. Department of Transportation. The technology that SwRI is applying to the detection of mechanical damage defects is known as nonlinear harmonics (NLH). NLH measures the changes in material magnetic properties as effects of stress and strain. Figure 1 illustrates the effects of applied stress on typical magnetic hysteresis curves. Note that tensile loading causes the curves to be steeper (increased magnetic permeability), while compressive loading yields an opposite result. The corresponding effects of plastic strain on the initial magnetization curves are shown in Figure 2. Note that the effects of compressive plastic strain are similar to applied tensile strain, i.e. an increased magnetic permeability.

The NLH method reveals the behavior of magnetic permeability at the surface of the metal part. Refer to Figure 3 that shows the basis of the NLH method. If an oscillatory magnetic field is impressed on a ferromagnetic workpiece, the magnetic field that is induced into the part is shaped by the hysteresis curve of the material. Since that curve is not linear, the magnetic induction is not a single-frequency sinusoid like the excitation waveform, but rather contains higher frequencies (harmonics) of the excitation frequency. Of particular interest are the odd harmonics, specifically the third. It has been shown in previous work at SwRI that the amplitude and phase of the third harmonic contain information about the amount of biaxial stress in the material.

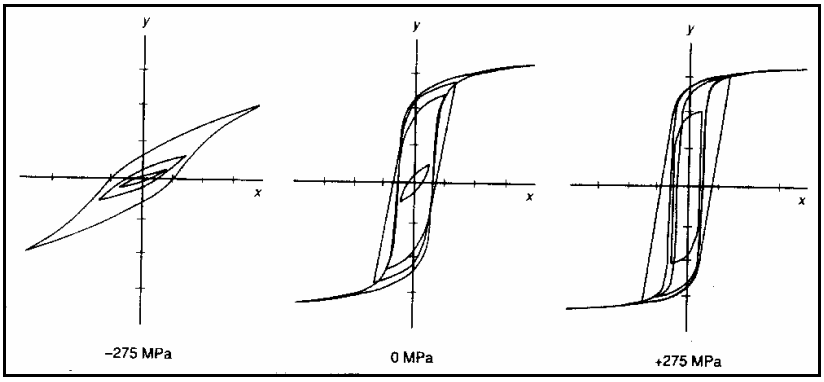

Figure 1: Magnetic properties vary with specimen loading.

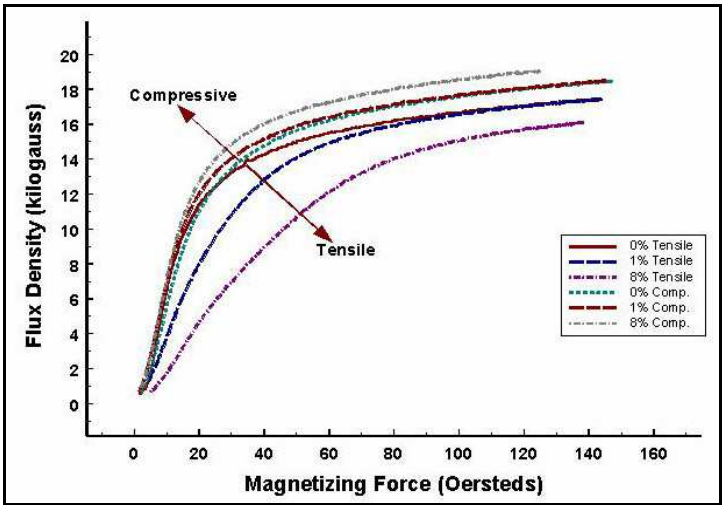

Figure 2: Initial curve and plastic strains.

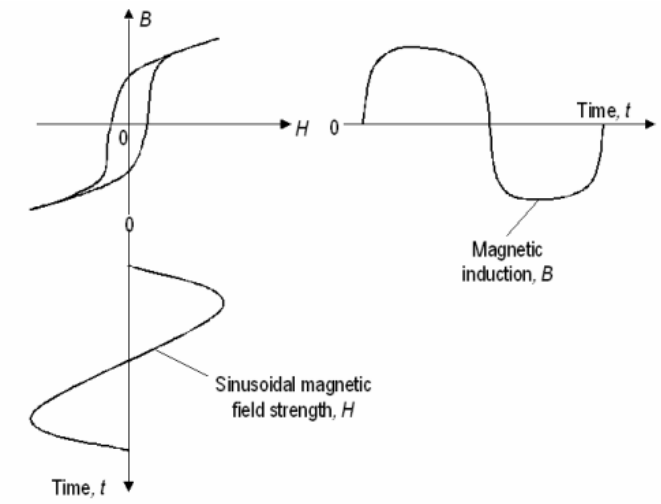

Figure 3: Basics of Nonlinear Harmonic Method.

The NLH probe is essentially a small ferrite-core transformer. When the core is placed against a ferromagnetic material, the material forms part of the transformer's magnetic circuit. Thus, the output of the transformer depends on the magnetic properties of the tested part. An NLH probe used by SwRI in research on mechanical damage defects is shown in Figure 4. Note that two windings are wound on the single C-shaped core. The required electronics are relatively simple, as shown in Figure 5. A sine-wave signal source, with power amplification, if needed, is connected to the probe's primary winding. The secondary sensing coil is first filtered to remove the fundamental frequency, leaving the higher harmonics that carry information about stress and strain. These harmonics are fed to a lock-in amplifier that is locked to the signal generator waveform, which makes it possible to observe amplitude and phase of a particular harmonic of the excitation waveform. In the mechanical damage detection work, the third harmonic was selected. Specifically, the excitation was 10 kHz, and the detected harmonic was 30 kHz. Since the sensing of magnetic properties takes place at 30 kHz, the sensing depth into the material is limited to a small fraction of a millimeter. Thus, an in-line inspection for outside mechanical damage relies on there being an effect at the inner surface. Of course if the defect is a dent, even a re-rounded dent, there was necessarily a disturbance of the inner surface. In addition, for a pressurized pipe, the stress field about an external gouge can extend to the internal surface.

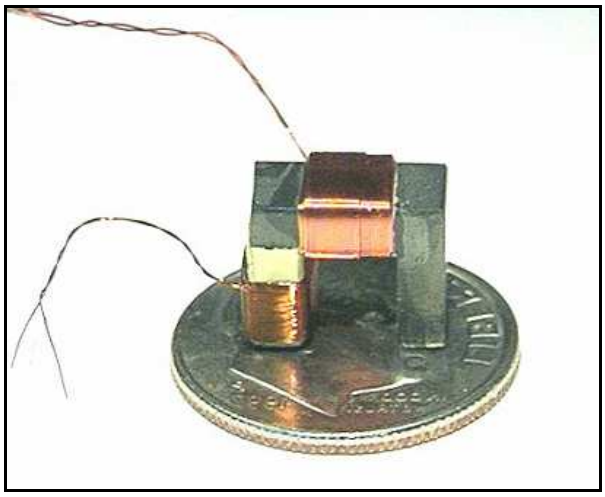

Figure 4: Typical NLH probe.

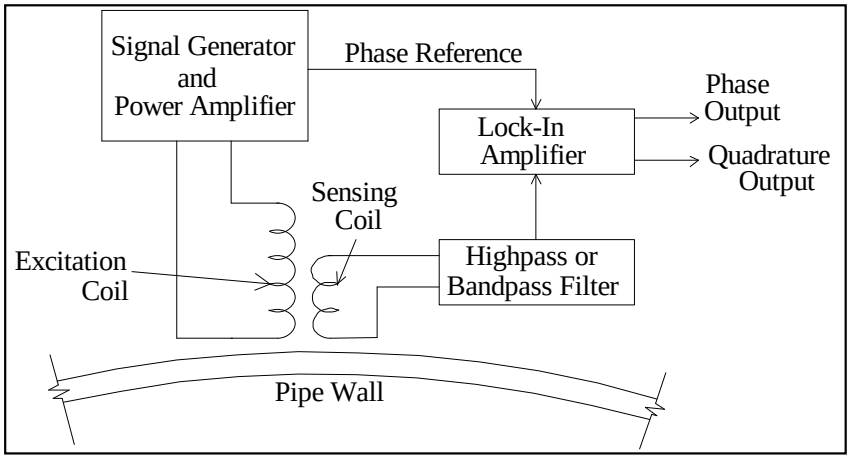

Figure 5: NLH circuit block diagram.

For gouged dents that do not fail immediately, the most common failure mode is the generation of cracks adjacent the external gouge and the growth of those cracks through the pipe wall with the resulting pipe failure. Crack initiation and growth are driven by the cyclic pressure variations inside the pipeline. This project was designed to evaluate the ability of NLH sensing to detect changes in gouged dents as the pipe was subjected to more and more cycles of internal pressure variation.

The critical work is being carried out on 2-meter long sections of 12-inch pipe. Defects were installed in the test sections using a machine that allows varying the loading and movement of an indenter. The defects are roughly similar to those caused by equipment such as backhoes. Gouges were produced at the center of dents of various depths.

Each of the test pipe sections has a flange neck on one end and a dome closure on the other. Penetrations through the blind flange end cap make it possible to control a scanner carrying NLH probes. Figure 6 shows a CADD drawing of the internal scanner. The probes are spring-loaded on a traveling "spider," which can be positioned at any point on the pipe inner surface by action of two computer controlled stepper motors on the face of the blind flange. One motor controls the circumferential position of the probes and the other the axial position. Thus, a scan pattern can be implemented to cover the area adjacent each defect.

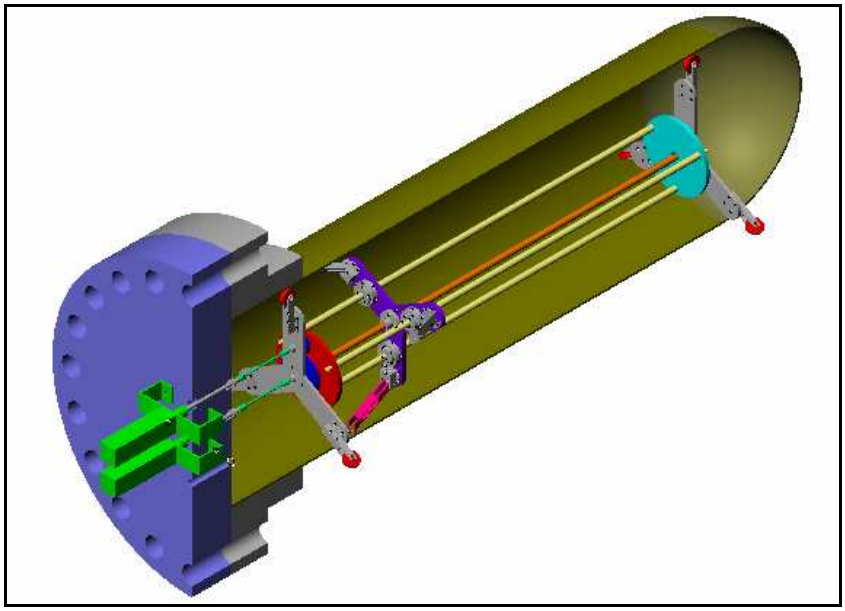

Figure 6: CADD drawing of internal pipe scanner for NLH during pressure testing.

NLH scans are being performed on four gouged pipes (pipe samples 2 through 5) subject to pressures of 1400 psi. Initial results for pipe samples 2 and 4 are shown in Figures 7 and 8. The scans were made using axial and circumferential fields, with the probes approximately 13 inches apart in the circumferential direction. Thus, in Figures 7 and 8, the circumferential length scales are offset by about 13 inches.

The scans are made around most of the circumference of the pipes (approximately 38 inches) and over an axial length of 52 inches. NLH scan measurements are made at axial intervals of 0.02 inch (2600 readings) and circumferential intervals of 0.25 inch (152 readings). The NLH signals were smoothed prior to plotting the results in Figures 7 and 8. This smoothing involved averaging the NLH signal over a small area [0.08 inch (axial) by 0.5 inch (circumferential)].

Figure 7 shows the NLH results for pipe sample 2. Several observations can be made (similar observations can be made about Figure 8 and pipe sample 4):

- Pipe 2 contained six intended defects, designated 2-1 through 2-6. The figures to the right in Figures 7(a) and (b) show maps identifying the locations of these defects. Table 1 details the gouge depths and sizes of the intended defects for the four pipes.
- Three unintended defects were observed on the outside of the pipe sample. These are identified by "*" signs on the defect map. These defects are attributed to cases when the first attempt at gouging produced defects that were considered too benign and left in the pipe or cases where the defects may have been introduced during practice attempts at fabricating gouges.
- A line of variable width corresponding to low NLH signal measurements is apparent on both the axial and circumferential field scans. This line physically corresponds with the seam weld that runs along the axis of the pipe. Thus, either due to magnetic property changes between weld and parent metal or residual strains resulting from the welding process, the NLH probes were able to detect the seam weld.
- The strain anomalies resulting from the intended defects, 2-1 through 2-6, were all detected by both the axial and circumferential field scans. (These defects are circled in Figure 7.
- Two of the unintended defects were also readily detected by the scans. The third unintended defect (adjacent to 2-6) was not detected. Visual inspections of the unintended defects indicated that the two defects that were detected (adjacent to 2-2 and 2-3) had surface lengths of 1.75 and 5 inches, widths of 0.375 and 0.375 inch, and depths of 0.250 and 0.062 inch, respectively. The undetected defect appeared to have a length of 2 inches and a width of 1.5 inches and could be characterized as a grind mark (its depth was not readily determinable). This defect appeared, therefore, to be benign.

The NLH scans on pipe sample 4 shown in Figure 8 also detected the six intended defects (designated 4-1 through 4-6) and one out of three unintended defects. The unintended defect that was detected (midway between 4-3 and 4-5) had a length of 2 inches, a width of 0.125 inch, and a depth of 0.062 inch. The two unintended defects that were not detected had lengths of 6.5 and 10 inches, widths of 2 and 3 inches, and depths that were too shallow to be determined. Thus, these two defects could be considered benign compared to the unintended defect that was detected.

Figure 9 compares plots of the circumferential field scan made over defect 2-4 (see Figure 7) with and without the smoothing procedure applied. It can be seen that the smoothing procedure produces a clearer image of the NLH signals with only apparent minor loss in detail. Table 1 contains the design data for the defects.

Table 1: Matrix of gouged dents fabricated in four pipe samples

Pipe No.	Gouge Sample Number	Gouge Depth (inches)	Gouge Depth (%, d/D)	Gouge Length (inches)	Gouge Tool	Wedge Width (inches)	Severity Factor
2	2-1	0.40	3.14	3	Rectangle	0.46	0.60
2	2-2	0.35	2.75	3	Wedge	0.33	0.42
2	2-3	0.50	3.92	1	Wedge	0.33	0.44
2	2-4	0.36	2.82	3	Rectangle	0.46	0.40
2	2-5	0.48	3.76	3	Square	0.75	0.98
2	2-6	0.48	3.76	1	Rectangle	0.46	0.31
3	3-1	0.65	5.10	3	Square	0.75	3.30
3	3-3	0.60	4.71	3.5	Wedge	0.33	4.57
3	3-4	0.70	5.49	2	Rectangle	0.46	3.19
3	3-5	0.70	5.49	2.5	Square	0.75	3.40
3	3-6	0.70	5.49	1.75	Wedge	0.33	3.16
4	4-1	0.55	4.31	4	Square	0.75	2.64
4	4-2	0.45	3.53	6	Rectangle	0.46	2.96
4	4-3	0.60	4.71	2	Rectangle	0.46	1.72
4	4-4	0.60	4.71	1.5	Wedge	0.33	1.41
4	4-5	0.50	3.92	6	Square	0.75	3.54
4	4-6	0.50	3.92	4	Wedge	0.33	2.72
5	5-1	0.50	3.92	4	Rectangle	0.46	2.30
5	5-2	0.60	4.71	2.5	Wedge	0.33	2.76
5	5-3	0.50	3.92	4	Wedge	0.33	2.72
5	5-4	0.55	4.31	3.5	Rectangle	0.46	2.73
5	5-5	0.60	4.71	3	Square	0.75	2.39
5	5-6	0.55	4.31	3	Wedge	0.33	2.55

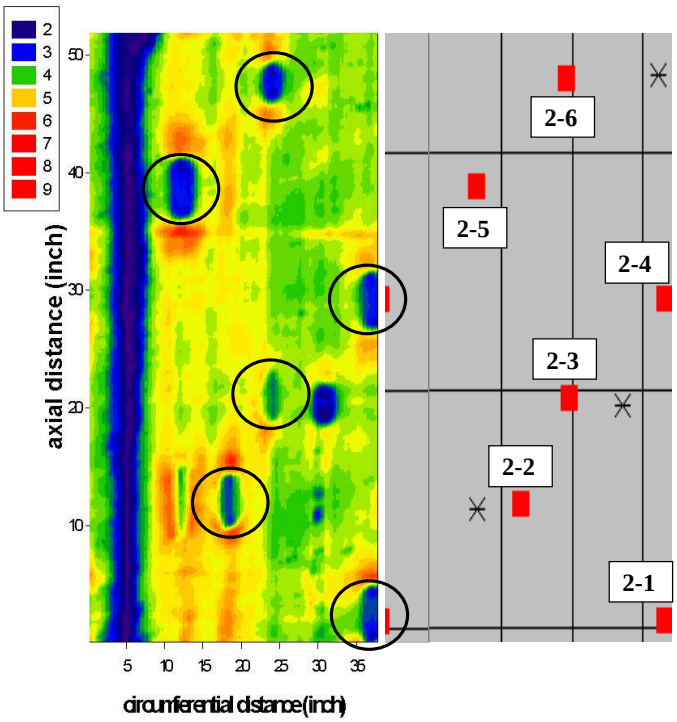

(a) axial field

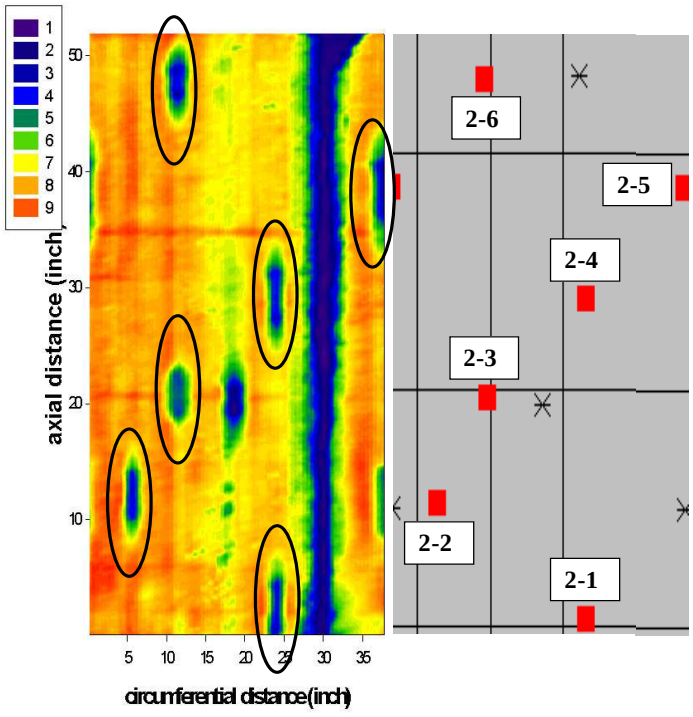

(b) circumferential field

Figure 7: Results of axial and circumferential NLH scans on pipe sample 2 pressurized to 1400 psi.

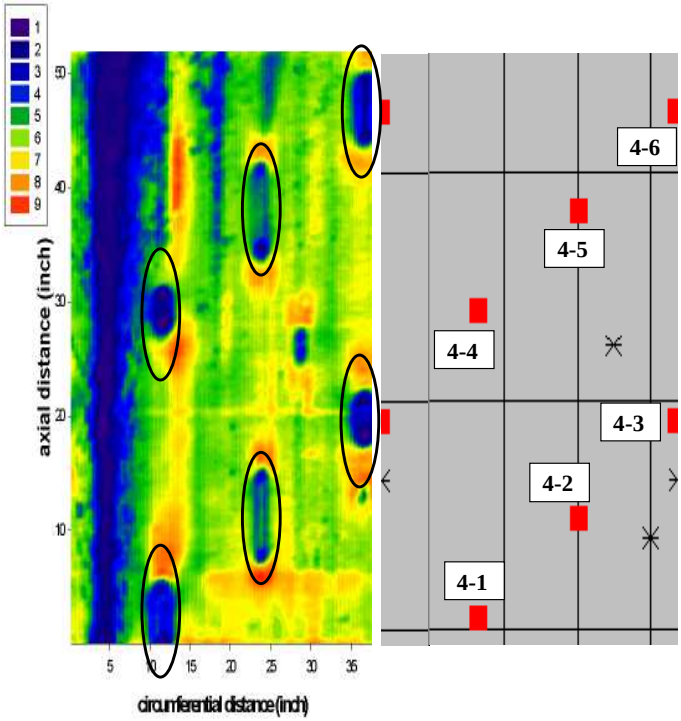

(a) axial field

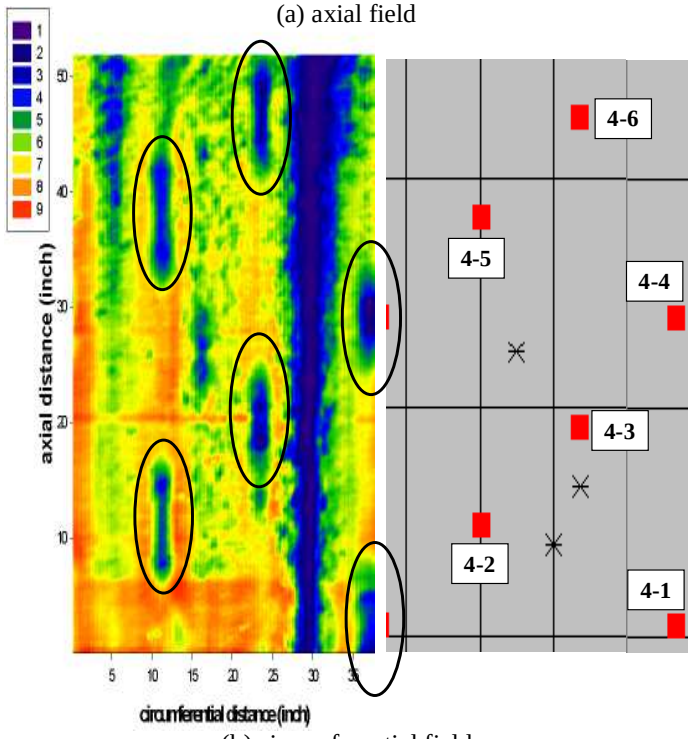

(b) circumferential field

Figure 8: Results of axial and circumferential NLH scans on pipe sample 4 pressurized to 1400 psi.

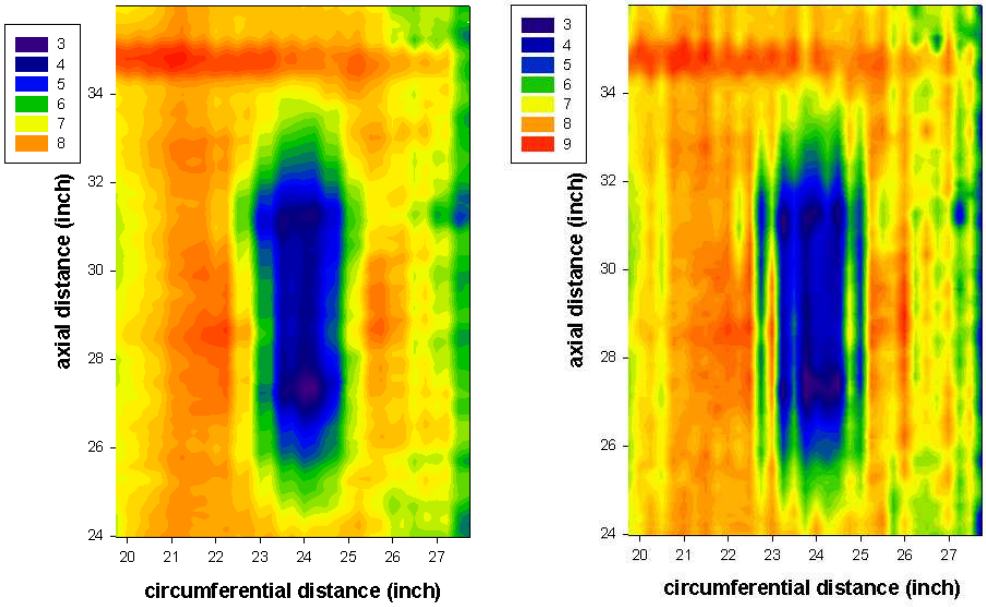

(a) Smoothed plot (b) Raw plot

Figure 9: Blow-up of circumferential field NLH signal results for defect 2-4 comparing a smoothed plot (a) with a plot based on the raw data (b).

Figure 10 shows typical NLH circumferential magnetic field scan results (magnitude and phase angle) for pipe samples 2 and 5. Maps contained in the figure illustrate the locations of the gouges in the pipes and whether they were intended or unintentional. (The unintentional defects were introduced in the pipes during trial gouge fabrication runs.) The strain anomalies on the insides of the pipes due to the gouges on the outsides are clearly visible from the NLH scans, as are the seam welds that run the axial lengths of the pipes. Interestingly, in the magnitude measurements, the seam welds manifest themselves as low voltage values (deep blue colored contours), whereas they produce high readings (red colored contours) in the phase angle measurements. The gouges also correspond to low voltage readings in the magnitude measurements, but appear as low regions surrounded by localized regions of high readings in the phase angle measurements.

Based on experience obtained during fabrication of the gouges in pipe samples 2 through 5, it is judged that defect 2-5 in pipe sample 2 is the severest of the six intended defects in this sample, and defect 5-6 is the fourth severest in pipe sample 5. It is also judged that all the defects in sample 5 are more severe than those in sample 2. To date, after application of over 10000 pressure cycles, none of the defects in sample 2 have failed (leaked), whereas, consistent with the severity rankings of the two pipe samples, four defects have failed in pipe sample 5. These are defects 5-4 (after 897 pressure cycles), 5-6 (after 5299 cycles) and 5-2 and 5-3 (each after 7769 cycles). (The empirical severity ranking procedure gave defects 5-4, 5-6, 5-2, and 5-3 similar severity ranking scores of 2.73, 2.55, 2.76, and 2.72, respectively, compared to scores of 2.30 and 2.39, respectively, for the two defects 5-1 and 5-5 that have not failed. Severity rankings of less than 1 were estimated for all the defects in sample 2. The severity score of defect 2-5 was 0.98.)

Figures 11 and 12 compare the NLH scan results for defects 2-5 and 5-6, respectively, as the number of pressure cycles experienced by each increased. There appear to be no clearly defined trends in either the NLH magnitude or phase angle measurements to indicate the accumulation of significant fatigue damage at either of the defects, this despite the fact that defect 5-6 failed after 5299 pressure cycles. However, there are differences in the measured NLH signals recorded after different numbers of pressure cycles, but how these are to be interpreted in terms of fatigue damage is not currently clear.

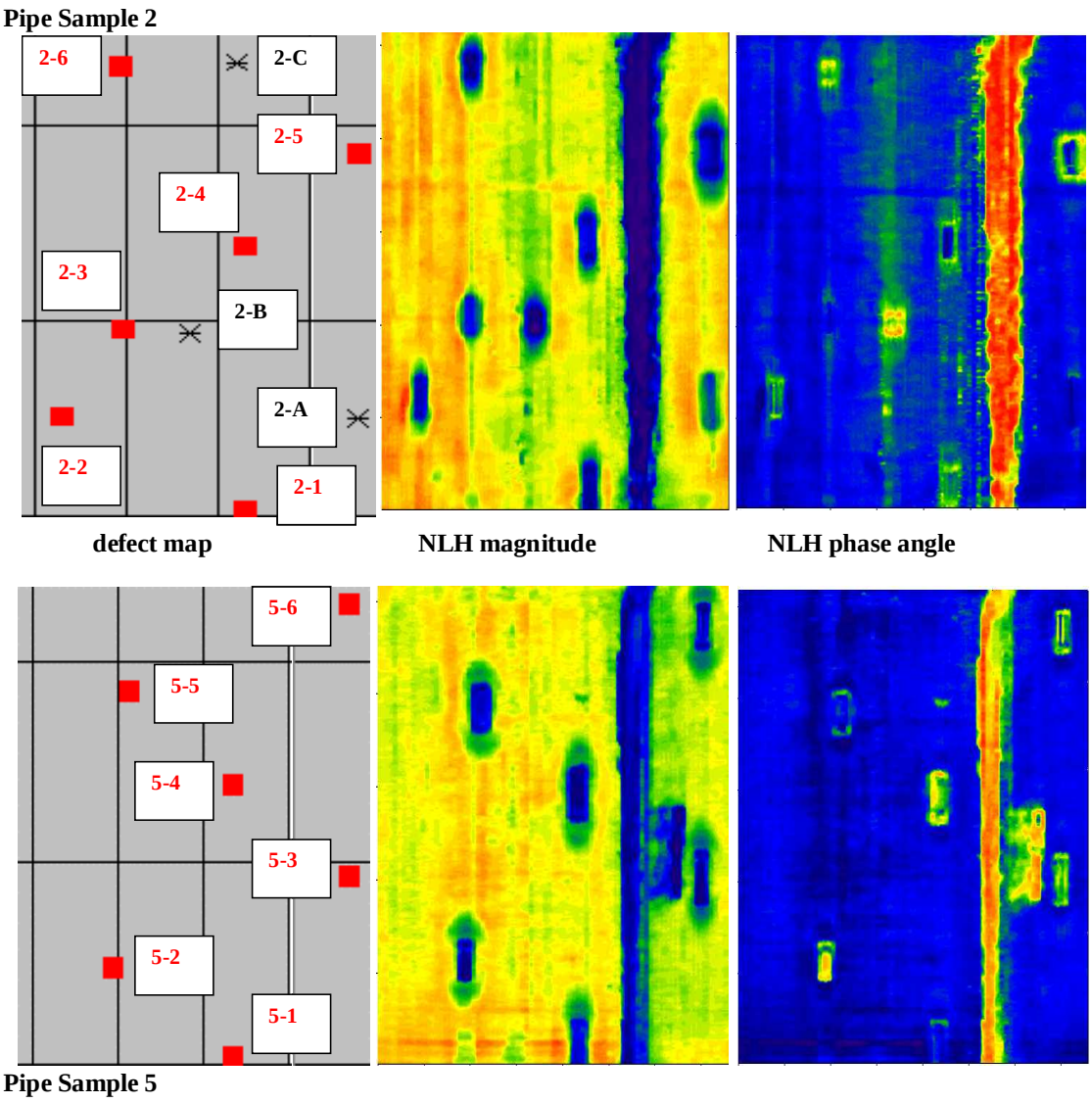

Figure 10: NLH circumferential magnetic field scan results for pipe samples 2 and 5 under 1400 psi pressure with the x-axis representing the circumference of the pipe (approximately 38 inches) and the y-axis the axial distance scanned (approximately 52 inches). The schematics on the right shown a map of the defect locations with the intentional defects signified in red and the unintended defects signified in black. The central and right hand figures show measured NLH magnitudes and phase angles, respectively.

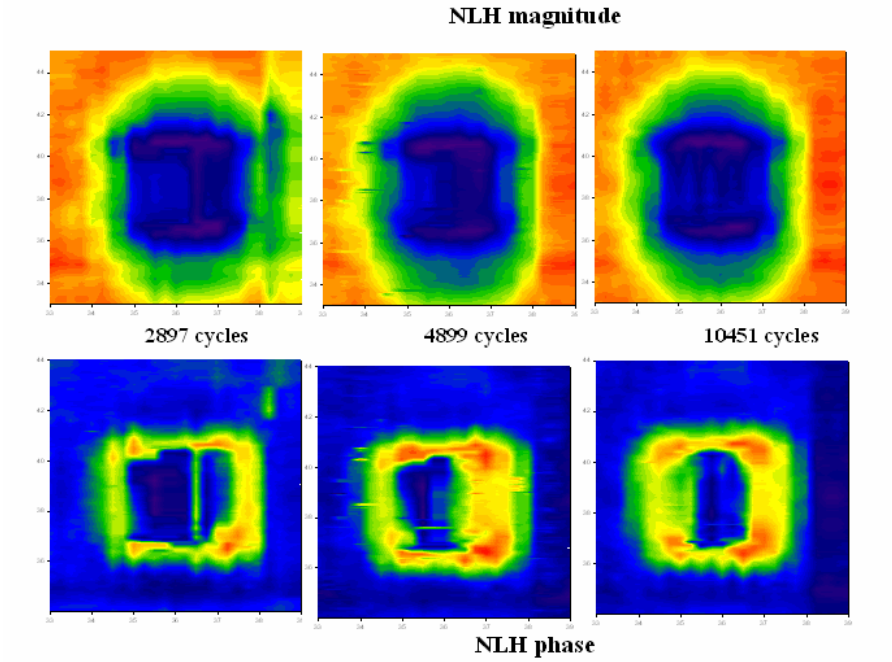

Figure 11: From left to right, NLH circumferential magnetic field scan results obtained for defect 2-5 in pipe sample 2 after 2897, 4899 and 10451 pressure cycles. The top figures are the measured NLH magnitudes, and the lower ones the NLH phase angles.

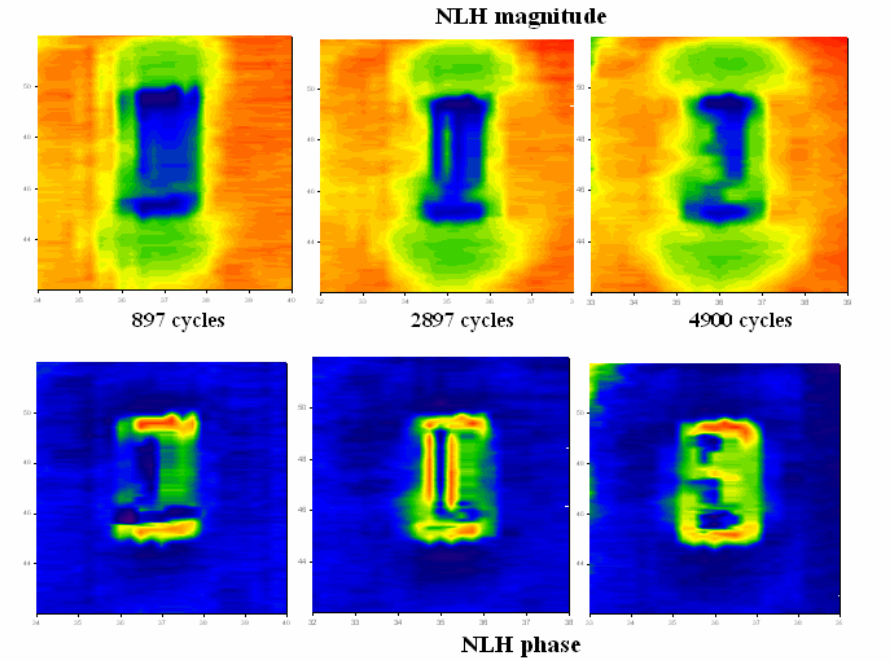

Figure 12: From left to right, NLH circumferential magnetic field scan results for defect 5-6 in pipe sample 5 after 897, 2897, and 4900 pressure cycles. The top figures are the measured NLH magnitudes, and the lower ones the NLH phase angles.

CONCLUSIONS

This paper describes work in progress. To date, all pipe specimens have been subjected to multiple steps of cyclic loading with NLH scans between steps. Several defects have failed by developing axial cracking that led to leaks. Analysis of NLH data is continuing, to determine whether the technique can reliably detect pipe wall changes that are precursors to failure.

ACKNOWLEDGMENTS

SwRI staff members who contributed to this work, besides the authors, include Senior Research Engineer Craig Redding, and Senior Technician Gary Hancock. Acknowledgment of the support of PHMSA's Jim Merritt and the Pipeline Research Council International is also appropriate.